Kazuyo Kobayashi Dias Franco, Margareth; Yokaichiya, Fabiano; Kardjilov, Nikolay; de
Oliveira Ferraz, Antonio Carlos
Microfocus X-ray imaging of Brazil nuts for quality control

Microfocus X-ray imaging of Brazil nuts for quality control

Imagens de Raios-X (Microfocus) no controle de qualidade de castanha do Brasil

Margareth Kazuyo Kobayashi Dias Franco[1*]; Fabiano Yokaichiya[2]; Nikolay Kardjilov[3]; Antonio Carlos de Oliveira Ferraz[4]

Abstract

Non-destructive quality assessment of food prior to processing is desirable in commercial facilities due to its non-invasive nature, for economic reasons and for its safety appeals. Grading Brazil nuts in this way allows for the separation of undesirable nuts to avoid contamination during the automatic nut-shelling process. The aim of this study was to evaluate the feasibility of X-ray phase contrast enhanced imaging in assessing nut quality. For this goal, details of the imaging technique are described and phase contrast X-ray and microtomography imaging of nut samples are investigated. Both high quality (i.e. "sound") nuts as well as treated nuts were examined. It was concluded that both the X-ray imaging and tomography techniques have the potential to discriminate morphological features of the nut and to identify "sound" kernels from atypical ones. Larger nuts and nuts with a larger gap area between shell and kernel were concluded to have more atypical formations. Both techniques also seemed promising for use in automatic sorting lines. However, by using microtomography, the visualization of finer formations not noticeable in the X-ray images was possible. Further studies shall be carried out to investigate the nature of these formations, how they affect nut quality and their evolution with storage time.

Key words: *Bertholletia excelsa*, fungus, microtomography, phase contrast, X-ray imaging

Resumo

Atualmente os grandes centros comerciais de processamento de alimentos buscam a avaliação prévia da qualidade dos produtos através de técnicas não destrutivas, devido aos apelos econômicos e de segurança alimentar. A classificação de castanhas-do-brasil através desta avaliação permite a separação das castanhas indesejáveis com a finalidade de evitar contaminações durante o processo de extração da amêndoa. O objetivo desse estudo foi avaliar a viabilidade do uso da imagem de raios-X, obtida através da técnica de contraste de fase para avaliação da qualidade da castanha. Para este objetivo, detalhes da técnica de são descritos e amostras de castanhas-do-brasil são investigadas pelas técnicas de imageamento por microtomografia e por contraste de fase de raios-X. São utilizadas castanhas saudáveis e castanhas tratadas, sendo estas últimas utilizadas com o objetivo de identificar modificações. Concluiu-se que ambas as imagens de radiografia e de tomografia de raios-X, apresentam um grande potencial para discriminar características morfológicas das castanhas e selecionar amostras saudáveis das tratadas.

[1] Pesquisador Dr., Instituto de Pesquisas Energéticas e Nucleares, IPEN, Reator Multipropósito Brasileiro, São Paulo, SP, Brasil. E-mail: mkfranco@ipen.br

[2] Pesquisador Dr., Department Quantum Phenomena in Novel Materials, Helmholtz Zentrum Berlim für Materialien und Energie GmbH, Hahn-Meitner-Platz 1 D-141 09 Berlin, Germany. E-mail: fabiano.yokaichiya@helmholtz-berlin.de

[3] Pesquisador Dr., Institut Angewandte Materialforschung, Helmholtz Zentrum Berlim für Materialien und Energie GmbH, Hahn-Meitner-Platz 1 D-141 09 Berlin, Germany. E-mail: kardjilov@helmholtz-berlim.de

[4] Prof. Dr., Faculdade de Engenharia Agrícola-FEAGRI, Universidade Estadual de Campinas, Cidade Universitária Zeferino Vaz, Campinas, SP, Brasil. E-mail: carlos@feagri.unicamp.br

[*] Author for correspondence

Dentro do conjunto de amostragem, castanhas grandes e castanhas que apresentam espaços maiores entre casca e amêndoa, mostraram formações atípicas. Ambas as técnicas mostraram-se também promissoras para serem utilizadas em linhas de produção automatizadas. Não obstante, através da microtomografia faz-se possível a visualização de características físicas mais detalhadas que não podem ser observadas usando as técnicas convencionais de imageamento de raios-X, como a radiografia convencional. A investigação da natureza destas formações, como elas afetam a qualidade das castanhas e sua evolução em função do tempo de armazenamento devem ser alvos de futuras investigações.

Palavras-chave: *Bertholletia excelsa*, fungos, micro tomografia, contraste de fase, imagem raios-X

Introduction

Nowadays, the quality control of food and agricultural products is necessary. Quality control needs to be highly accurate, be fast and be capable of objective assessment. In Brazil, nuts collected from the Amazon forest are not subjected to automated quality process control. Control operations are generally unreliable due to subjective decisions in quality assessment using attributes such as appearance, flavor and texture. The Brazilian nut (*Bertholletia excelsa* H. & B. – *Lecythidaceae*) harvesting is an example of this extractivism. As the second major world producer after Bolivia, Brazil produced 19 340 tons of Brazil nuts in 2011. Of this amount, 24% was exported to Europe, China and Bolivia (NEVES et al., 2012). Brazil focuses its marketing and commercialization on the actual nuts, while Bolivia focuses more on the kernels. In this framework, the development of non-destructive techniques for characterization and quality control of Brazil nuts is important as a way of offering high quality products worldwide.

Many non-destructive techniques are already available to characterize agricultural products (KARUNAKARAN et al., 2004: PATEL et al., 2012). The extensive use of soft X-ray techniques in the fruit and vegetable industry is well-known to determine maturity levels; to detect internal voids, insect damages and foreign material in foods (DIENER et al., 1970; HAN et al., 1992). Characterization of grain kernels such as dormancy, viability and internal damages have been carried by soft X-rays (CICERO et al., 1998).

Researchers have devoted great efforts to the application of non-destructive methods (NUGENT et al., 1996) for obtaining high-resolution X-ray images. These non-destructive quality assessment methods may be useful in the characterization and inspection of food composites before processing at an industrial scale (YANNIOTIS et al., 2011; DONEPUDI et al., 2013; THOMAS et al., 1995). The images are used to inspect the interior of specimens, and contrast can be seen when different physical properties are present. Normal tabletop X-ray sources can obtain images based on the absorption of the sample, where contrast comes from the medium atomic number (VAN DER BURG et al., 1994; CICERO et al., 1998). Recently, the advent of a new generation of X-ray tubes, with a high intensity, small emitting area and high-resolution X-ray cameras made possible the observation of some coherent effects in the X-ray imaging setups (GUREYEV et al., 1996). Common in visible optics, single point imaging and microscopy consists of observing the image projection or shadow levels from a sample illuminated by a quasi-punctual light source (Figure 1a, 1b) (SPENCE, 2007).

Recent advances using microfocussed X-ray sources enabled phase contrast enhanced X-ray images suitable for industrial applications. Considerable research has been performed in advancing this type of imaging technique. In addition, its importance as a defect and inspection tool for specific features and new applications is growing fast in several areas such as food processing, cement compound analysis and microbiology (THOMAS et al., 1995; NOGUEIRA et al., 2010).

Since these images are obtained with the same radiological path as a normal absorption image, computed tomography can be used to produce three-

dimensional reconstructions and therefore new types of results could be found with this imaging method. Three-dimensional microtomography reconstruction of the object requires a data processing algorithm for segmentation and viewing. The reconstruction is based on multiple images obtained from the same object, rotated at regular intervals. A tomography is generated by filtered back projection of these images (SLANEY; KAK, 1985).

As discussed above, the study of the viability of phase contrast imaging techniques in biological specimens, such as *Bertholletiaexcelsa,* is relevant because it improves the visibility of finer structures in the sample, in a non-destructive way. Phase contrast image allows one to examine details and edge effects, which is not possible when using conventional X-ray imaging (DAVIS et al., 1995).

Therefore, the objectives of this study were: (1) to investigate X-ray phase contrast enhanced imaging and X-ray microtomography techniques to inspect the quality of the Brazil nut; (2) to use image line profiles to determine morphological features of the nuts.

Figure 1. a) Experimental setup for microfocus X-ray imaging. b) Different regimes of imaging using phase contrast enhancement by a quasi-punctual X-ray source.
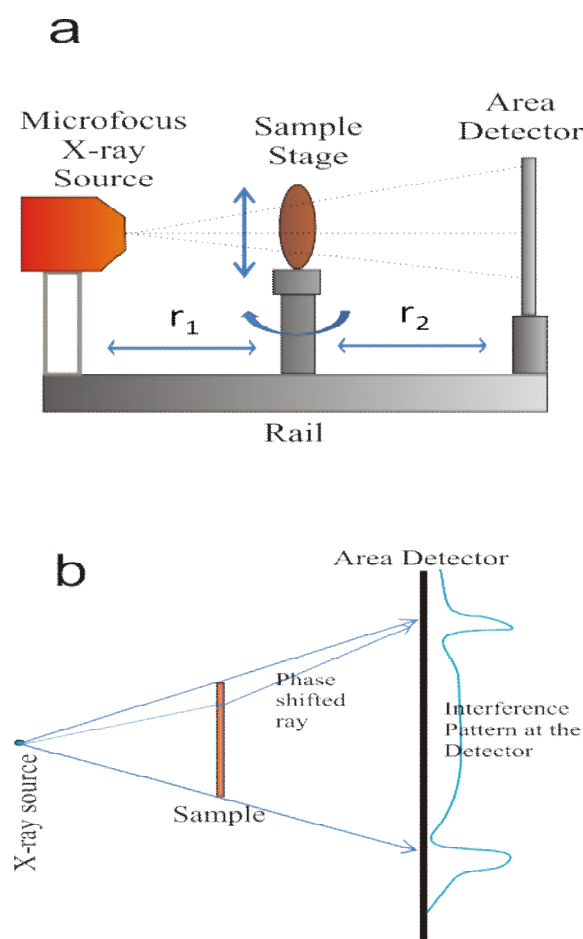
Materials and Methods

Sample treatment

We selected two sets of Brazil nuts (*Bertholletia excelsa*) that were commercially available in the Brazilian market, each one containing 50 to 100 fresh nuts. One of the sets had nuts of high quality, determined via a visual inspection. The other set was sprayed with water and kept for a two week period in a dark environment, at 35 °C and 80% relative humidity. After this period, visible fungus partially covering the nut shells was observed; it is important to note that this may not guarantee that the inside, i.e. the kernel, was contaminated.

X-ray imaging and microfocus setup

Nut X-ray images were acquired using a setup (Figure 1) that allowed for phase contrast enhancement using a Hamamatsu microfocus X-ray source (L9191-02) with a 5 µm in diameter emission spot tungsten target (HAMAMATSU, 2012). These features allowed us to obtain X-ray beams in the 40 to 130 KeV energy range. Positioning the detector 1 m away from the source provided an estimated lateral coherence of 20 µm, which allowed for the enhancement of specimen features that had dimensions of less than 20 µm.

Two detectors were used: a 48 µm pixel resolution Rad-Icon Shad-o-Box 4k (2048x2048 pixels), for the acquisition of the phase contrast images at high resolution; and a 22.5µm resolution Rad-Icon Rad-Eye HR (1200x1600 pixels), to obtain the microtomography image sets (RAD-ICON, 2012). Both detectors are highly sensitive to X-ray energies of 20 to 130 KeV. The setup was hosted at the Laboratory of Applied Crystallography and X-ray, University of Campinas (UNICAMP), Brazil.

The sample stage (Figure 1) was composed of a sample holder and a motor-controlled vertical and angular positioning device, which enabled sample manipulation for image acquisition.

To obtain the nut images and microtomography (µCT), the distances between source and object and between object and detector, maximum emission voltage, current and acquisition time of each image were optimized. This was done in order to maximize the signal to noise ratio and the image contrast.

Tomography setup

The µCT X-ray setup used at Helmholtz-Zentrum Berlin consisted of a micro-focus 150 kV Hamamatsu X-ray source with a tungsten target and a flat panel detector C7942 (120x120 mm^2, 2240x2368 pixel^2, pixel size 50 µm). The principle of the cone beam imaging system is shown in Figure 1. A 120 kV filament voltage and a current of 83 µA with an exposure time of 1.4 s per angular projection were used for the scan. The source-object distance was 250 mm and the source-detector distance was 550 mm, thus achieving a magnification factor of 2.2 which reflected in a voxel size of 23 µm. The number of acquired projections was 1000, which yielded a total scanning time of 1 h approximately. Commercially-available software (Octopus V8.6) was used to perform the tomographic reconstruction, which was based on a back-projection algorithm with convolution and correction for cone beam.

Images and analysis

Images originated from a phase contrast radiography technique which utilized transverse coherent beams, and were captured in the Fresnel diffraction state (SNIGIREV et al., 1995). The images represent the sample attenuation coefficients' bi-dimensional distribution and they were captured due to the changes in the optical path of the beam that altered the wave phase in a way that the X-rays were subject to constructive and destructive interference. Thus, the images represent the intensity of the X-rays that went through the sample and reached the detector, which in turn represents different attenuation coefficients and different thicknesses.

The radiographic images were first treated to enhance contrast between object and background. To adjust visual image quality, corrections in brightness, contrast and gamma (non-linear operation to encode or decode luminance in video or image systems) were performed. Subsequently, image filtering was performed using the local equalization filter to improve border contrast and to reveal details in the lighter and darker regions. Finally, the areas of interest in the central cross-section plane of the nut were quantified by pixel counting and atypical formation spots were identified because they had the same intensity levels. For both procedures, the software ImageJ (SCHNEIDER et al., 2012) was utilized. The measured areas were nut (whole cross-section), kernel, and gap (inside nut space between kernel and shell). Kernel and shell discontinuities were not taken into consideration. An occupancy index defined as the rate between nut area and nut plus gap areas, varying from 0 to 1, was proposed in an attempt to discriminate between "sound" and treated nuts.

Results and Discussion

Phase contrast enhanced imaging

After a number of trials, the optimized parameters for best contrast in the set of radiographies were found to be 80 keV, 60 µA, 200 mm between source and sample, 400 mm between sample and detector and a 6 s exposure. Because of these settings, a three times image magnification factor was obtained.

X-ray phase contrast imaging allowed for discrimination of morphological features of the nut such as shell and kernel and also allowed us to identify the gap between the kernel and endocarp. It was also possible to identify structural kernel changes. Figure 2a illustrates an X-ray image of a good quality, non-contaminated Brazil nut, exhibiting kernel grayscale homogeneity as confirmed through visual inspection. On the other hand, in the treated batch, structural changes or atypical formations were easily identified, as indicated by the arrows in Figure 2b.

Figure 2. a) X-ray image of a "sound" nut. b) Treated nut showing modified kernel structures.
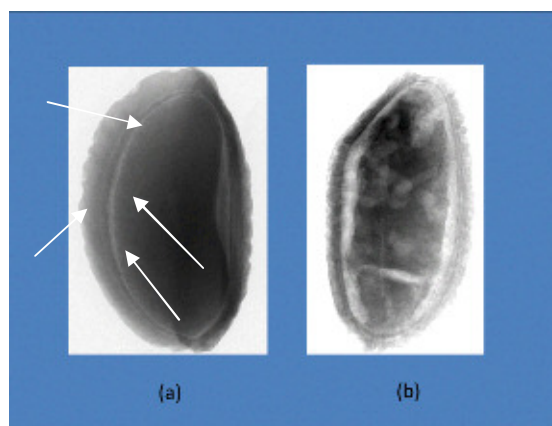
Temperature and high relative humidity affected the specimens in various degrees of severity, from mild to intense, indicated by the number of atypical formations in the kernel (Figure 3a). Since the gray level intensity indicates how much X-ray radiation was absorbed by the sample, we can clearly observe different structures in the kernel. A plot of the image gray level (Figure 3b) shows that peaks 1 and 4 are attributed to the gap between kernel and shell (Figure 3a), while the signal contrast illustrated by peaks 2 and 3 (Figure 3b) corresponds to specific atypical regions that are clearly identified by the lighter spots (Figure 3a). A detailed signal analysis of the images showed a relatively high contrast in atypical formation regions when compared to "sound" nuts (Figure 3c).

Figure 3. a) Enlarged view of an intense atypical kernel formation. b) Gray level count plot for the selected horizontal line along the nut is shown in (a). c) Gray level count for a typical "sound" nut.


(a)   (b)   (c)
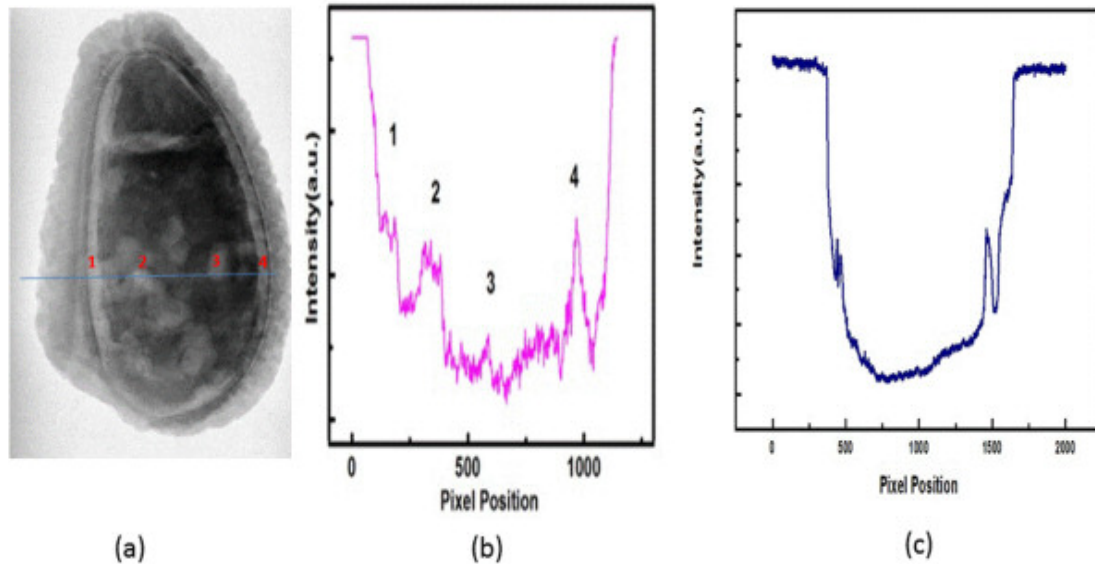
Another example of structural changes from a whole nut characterized by X-ray imaging, is shown in Figure 4. Figure 4a shows some heterogeneity in the grayscale indicating a structural change, verified through a visual inspection of the nut that had been cut open (Figure 4b).

As can be seen for a specific line (Figure 3b), the intensity level of the nut image is slightly parabolic. After image flattening, followed by threshold and binary conversion of desired features, such as nut, kernel and gap areas were extracted. The results (Tables 1 and 2) for the calculated areas show that the gap area is likely to have high coefficient of variation values of 21.50 and 57.18% for "sound" (non-treated) and treated nuts, respectively.

However, the kernel occupancy values showed small coefficient of variation values of 2.36 and 8.97%, for "sound" and treated nuts, respectively,

indicating the potential of the occupancy values to be used as an index to discriminate these two classes of nuts. In Figure 5, we show a plot of the kernel occupancy (kernel area divided by kernel plus gap area) versus kernel area. These areas were calculated by counting the number of pixels, obtained by using the binary conversion described above, multiplied by pixel area. From the plot, it was clear that larger nuts and large gap areas seem to make the nut more vulnerable to atypical formations. This correlation becomes important considering that bigger gaps contain more oxygen and moisture, which may encourage fungi development. The plot (Figure 5) shows three regions: "sound" nut region, poor quality (treated) nut region, and undefined region. These findings may help in the development and implementation of a system to select Brazil nut automatically.

Figure 4. a) X ray imaging. (b) Corresponding photograph of damaged nut kernel that has been cut open.
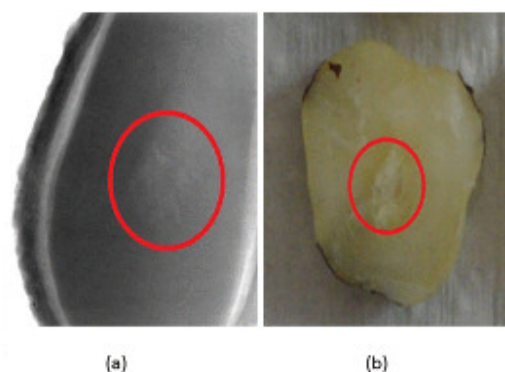
Table 1. Measured values of central cross-sectional areas of the nut, kernel, kernel and gap, gap and kernel occupancy (kernel and kernel + gap ratio) for "sound" nut using radiographic images.

Nut #	Nut (pixels)	Kernel (pixels)	Kernel + Gap (pixels)	Gap (pixels)	Kernel Occupancy	Kernel (mm^2)
01	944469	611808	703465	91657	0.86	439.7
02	881298	594630	657339	62709	0.90	410.8
03	934264	625128	676275	51147	0.92	422.7
04	991564	713983	780654	66671	0.91	487.9
05	868290	485283	537222	51939	0.90	335.8
06	982503	554706	611123	56417	0.91	381.9
07	822145	454989	515114	60125	0.88	321.9
08	775932	508554	590307	81753	0.86	368.9
09	873321	533637	586938	53301	0.91	366.8
10	1010598	607607	672345	64738	0.90	420.2
11	1013881	555087	631268	76181	0.88	394.5
12	1043507	620037	704300	84263	0.88	440.2
13	961115	628521	702315	73794	0.89	438.9
14	982463	482208	527703	45495	0.91	329.8
15	979171	567073	629201	62128	0.90	393.2
16	1032252	542545	631730	89185	0.86	394.8
17	1050573	511188	581512	70324	0.88	363.4
18	1043211	516072	603716	87644	0.85	377.3
19	988432	614151	706311	92160	0.87	441.4
Mean	956788.9	564589.8	634149.4	69560	0.89	396.3
C.V. *(%)	8.23	11.48	11.03	21.50	2.36	11.04

*Coefficient of variation.

Table 2. Measured values of central cross-sectional areas of the nut, kernel, kernel and gap, gap and kernel occupancy (kernel and kernel + gap ratio) for treated nuts using X-ray radiographic images.

| Nut #	Total nut (pixels)	Kernel (pixels)	Kernel + Gap (pixels)	Gap (pixels)	Kernel Occupancy	Kernel (mm^2)
01	1457106	1058436	1105599	47163	0.96	552.8
02	1116279	777777	892348	114571	0.87	446.2
03	1210006	669362	763851	94489	0.88	381.9
04	1501631	781075	876340	95265	0.89	438.2
05	1479411	692205	893290	201085	0.77	446.6
06	1202315	494295	785313	291018	0.63	392.6
07	1354744	847872	912676	64804	0.93	456.3
08	1174847	661796	744461	82665	0.89	372.2
09	1751597	1042750	1111100	68350	0.94	555.5
10	1399404	822270	1013616	191346	0.81	506.8
11	1595114	940907	1139103	198196	0.83	569.5
12	1457209	1020395	1024635	4240	0.99	512.3
13	1436575	814783	950720	135937	0.86	475.4
14	1021213	693577	765752	72175	0.91	382.9
15	1507660	865638	950611	84973	0.91	475.3
16	920867	631497	722311	90814	0.87	361.1
17	1497110	883018	1009713	126695	0.87	504.8
17	1213550	655776	781867	126091	0.84	390.9
19	1567397	952035	1058632	106597	0.90	529.3
20	1390386	879729	999346	119617	0.88	499.7
Mean	1361265	805550.7	921154.6	115603.9	0.87	460.6
C.V.* (%)	15.71	19.26	14.62	57.18	8.97	14.62

*Coefficient of variation.

Figure 5. Occupancy rate versus Kernel Area.
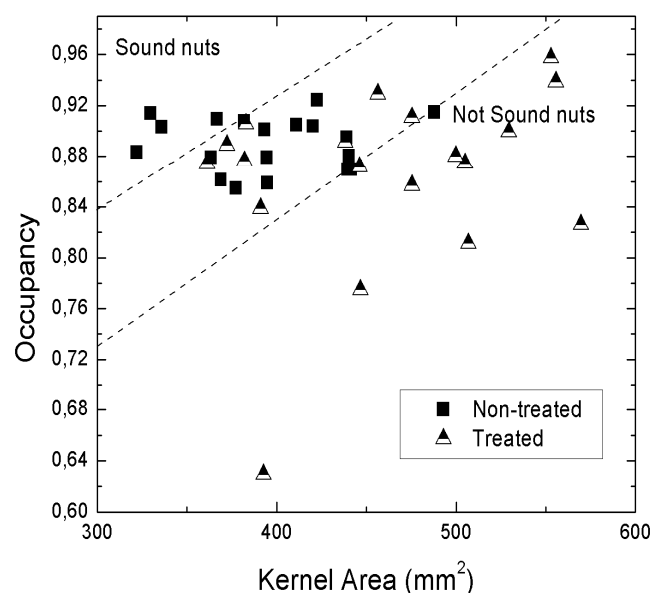
Phase contrast microtomography

With CT reconstruction, morphological features were also identified. However, μCT technique allowed us to observe the occurrences of structures that were not seen in individual phase contrast enhanced images, as previously discussed. Figure 6 shows a typical formation of a "sound" nut on the CT reconstruction. We can observe common morphological details such as the nut shell, kernel and holes inside the kernel. In contrast to the traditional image techniques, like radiography, μCT technique allows for identification of small dots in several slices, consisting of structural changes that could be attributed to chemical decomposition of lipids themselves or as a consequence of the presence of fungus.

**Figure 6**. X-ray microtomography reconstruction of a Brazil nut.
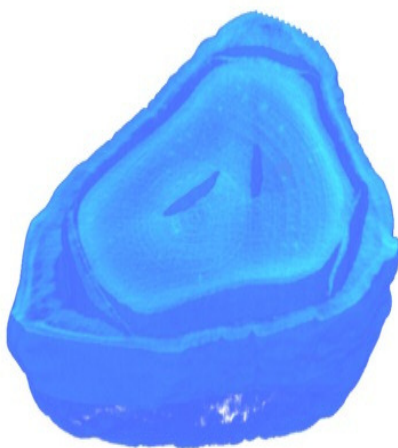
Moreover, in the same batch, Figure 7b shows a tomography slice from a nut that did not display any anomalous structures. On the other hand, Figure 7c shows a slice of the tomography from a treated (poor quality) nut.

The concept of anomalous density as being a structural change formation was conceived as feasible after carefully inspecting the tomography slices and nuts. However, we believe further investigations are necessary to determine the composition of these fine structures. These features are only visible in computed microtomography because of signal to noise ratio improvement, since more statistical data are collected with this method in comparison with a single image of the same sample (Figure 7a).

Figure 7e illustrates a line profile plot in atypical formation and the surrounding area, enlarged in Figure 7d, representing the voxel (3D pixel) intensity of a line crossing the center of one specific anomalous structure. Once the voxel intensity of a reconstructed tomography is proportional to the sample density, at that point, we can observe that the atypical formation mentioned above is 30% denser than its surroundings.

Figure 7. a) Radiographic projection of nut displayed in Figure 6. b) Tomography slice from another nut displaying an homogeneous kernel. c) Tomography slice from nut. d) Tomography slice showing an anomalous dot enlarged in the inset. e) Plot of tomography reconstruction density for one of the anomalous dots enlarged in (d).
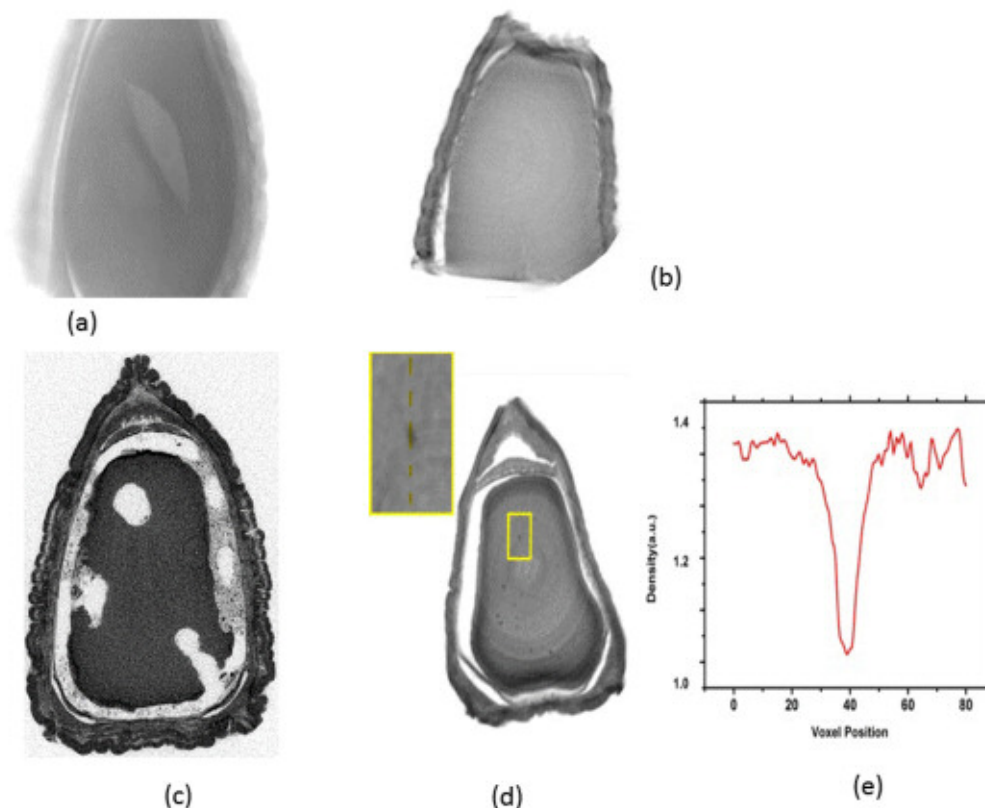
Conclusion

It was concluded that both, X-ray phase-enhanced imaging together with X-ray phase enhanced imaging microtomography, have the potential to differentiate morphological nut features and atypical formations in Brazil nut kernels. However, microtomography allowed for the visualization of finer formations not visible in the X-ray images. The techniques also seem promising for automatic sorting of the nuts due to their simplicity and low cost. Further studies are recommended to investigate the nature of the observed formations, how they affect nut quality and the evolution of nut quality with storage time.

Acknowledgements

References

CICERO, S. M.; VAN DER HEIJDEN, G. W. A. M.; VAN DER BURG, W. J.; BINO, R. J. Evaluation of mechanical damage in seeds of maize by X-ray and digital imaging. *Seed Science and Technology*, Zürich, v. 26, n. 3, p. 603-612, 1998.

DAVIS, T. J.; GAO, D.; GUREYEV, T. E.; STEVENSON, A.; WILKINS, S. W. Phase contrast imaging of weakly absorbing materials using hard x-rays. *Nature*, London, v. 373, n. 6515, p. 595-598, 1995.

DIENER, R. G.; MITCHELL, J. P.; RHOTEN, M. L. Using X-ray image scan to sort bruised apples. *Agricultural Engineering*, v. 51, n. 6, p. 356-357, 1970.

DONEPUDI, V. R.; BHASKARAIAH, M.; CESAREO, R.; BRUNETTI, A.; AKATSUKA, T.; YUASA, T.;

ZHONG, Z.; TAKEDA, T.; GIGANTE, G. E. Diffraction-enhanced imaging systems to image walnut at 20 keV. *Journal of Food Measurement and Characterization,* New York, v. 7, n. 1, p. 13-21, 2013.

GUREYEV, T. E.; EVANS, R.; STUART, S. A.; CHOLEWA, M. Quasi-one-dimensional tomography. *Journal of the Optical Society of America A-Optics Image Science and Vision*, Washington, v. 13, n. 4, p. 735-742, 1996.

HAMAMATSU. *Hamamatsu photonics*. Hamamatsu, 2012. Available at: <http://sales.hamamatsu.com/assets/pdf/parts_L/L9181-05_TXPR1004E01.pdf>. Accessed at: 27 june 2012.

HAN, Y. J.; BOWERS III, S. V.; DODD, R. B. Nondestructive detection of split-pit peaches. *Transactions of the ASAE*, Michigan, v. 35, n. 6, p. 2063-2067, 1992.

KARUNAKARAN, C.; JAYAS, D. S.; WHITE, N. D. G. Identification of Wheat Kernels damaged by the Red Flour Beetle using X-ray images. *Biosystems Engineering*, London, v. 87, n. 3, p. 267-274, 2004.

NEVES, G. A. R. *Influência do vapor sob pressão e radiação infravermelha no desempenho da decorticação, qualidade do óleo e resistência mecânica da amêndoa de castanha do Brasil.* 2012. Tese (Dissertação de Mestrado em Engenharia Agrícola) – Universidade Estadual de Campinas, Campinas.

NOGUEIRA, L. P.; BRAZ, D.; BARROSO, R. C.; OLIVEIRA, L. F.; PINHEIRO, C. J. G.; DREOSSI, D. 3D histomorphometric quantification of trabecular bones by computed microtomography using synchrotron radiation. *Micron*, London, v. 41, n. 8, p. 990-996, 2010.

NUGENT, K. A.; GUREYEV, T. E.; COOKSON, D. F.; PAGANIN, D.; BARNEA, Z. Quantitative phase imaging using hard x-rays. *Physical Review Letter,* College PK USA, v. 77, n. 14, p. 2961-2964, 1996.

PATEL, K. K.; KAR, A.; JHA, S. N.; KHAN, M. A. Machine vision system: a tool for quality inspection of food and agricultural products. *Journal Food Science Technology*, USA, v. 49, n. 2, p. 123-141, 2012.

RAD-ICON. Rad-icon imaging. Waterloo, 2012. Available at: <http://www.rad-icon.com>. Accessed at: 27 june 2014.

SCHNEIDER, C. A.; RASBAND, W. S.; ELICEIRI, K. W. NIH Image to imageJ: 25 years of image analysis. *Nature Methods*, London, v. 9, n. 7, p. 671-675, 2012.

SLANEY, M.; KAK, A. C. *Principles of computerized tomographic imaging.* New York: IEEE Press, 1985. 344 p.

SNIGIREV, A.; SNIGIREVA, I.; KOHN, V.; KUZNETSOV, I. On the possibilities of X-ray phase contrast microimaging by coherent high-energy synchrotron radiation. *Review Sciencetific Instruments*, New York, v. 66, n. 12, p. 5486-5492, 1995.

SPENCE, J. C. H. *Science of microscopy*. New York: Springer, 2007. 696 p.

THOMAS, P.; KANNAN, A.; DEGWEKAR, V. H.; RAMANURTHY, M. S. Non-destructive detection of seed weevil infested mango fruits by X-ray imaging. *Postharvest Biology and Technology*, London, v. 5, n.1, p. 161-165, 1995.

VAN DER BURG, W. J.; AARTSE, J. W.; VAN ZWOL, R. A.; LINK, H. J. A.; BINO, R. J. Predicting Tomato seedling Morphology by x ray analysis of seeds. *Journal of the American Society Horticultural Science,* Alexandria, v. 119, n. 2, p. 258-263, 1994.

YANNIOTIS, S.; PROSHLYAKOV, A.; REVITHI, A.; GEORGIADOU, M.; BLAHOVEC, J. X-ray imaging for fungal necrotic spot detection in pistachio nuts. *Procedia Food Science*, Athens, v. 1, n. 1, p. 379-384, 2011.